Three-loop correction to the instanton density. II. The sine-Gordon potential

M. A. Escobar-Ruiz, E. Shuryak, and A. V. Turbiner

Phys. Rev. D **92**, 025047 — Published 29 July 2015

DOI: 10.1103/PhysRevD.92.025047

Three-loop Correction to the Instanton Density. II. The Sine-Gordon potential

M.A. Escobar-Ruiz[1],* E. Shuryak[2],† and A.V. Turbiner[1,2‡]

[1] *Instituto de Ciencias Nucleares, Universidad Nacional Autónoma de México,*

Apartado Postal 70-543, 04510 México, D.F., México and

[2] *Department of Physics and Astronomy,*

Stony Brook University, Stony Brook, NY 11794-3800, USA

Abstract

In this second paper on quantum fluctuations near the classical instanton configurations, see [1], we focus on another well studied quantum-mechanical problem, the one-dimensional Sine-Gordon potential (the Mathieu potential). Using only the tools from quantum field theory, the Feynman diagrams in the instanton background, we calculate the tunneling amplitude (the instanton density) to the three-loop order. The result agrees (in six significant figures) with the one given long ago by J. Zinn-Justin using Schrödinger equation. As in the double well potential case, we found that the largest contribution is given by the diagrams originated from the Jacobian. We again observe that in the three-loop case individual Feynman diagrams contain irrational contributions, while their sum does not.

*Electronic address: mauricio.escobar@nucleares.unam.mx

†Electronic address: edward.shuryak@stonybrook.edu

‡Electronic address: turbiner@nucleares.unam.mx,alexander.turbiner@stonybrook.edu

Introduction

Since it is our second paper of the series, following the one on the double-well potential [1], it does not need an extensive introduction. Topological solitons, instantons in particular, are widely used in the context of quantum field theories and condense matter physics. Their relation to standard perturbative series is an old issue, which continues to produce interesting results, so far mostly in quantum mechanical context.

The Sine-Gordon (SG) field has been extensively studied in classical context, with an enormous literature dedicated to it, see e.g. [2] and references therein. Coleman [3] has extended the results to the quantized theory by relating the SG field to the zero-charge sector of the massive Thirring model. Also in [4] the explicit calculations for the tunneling amplitude using the so-called nonvacuum instantons at finite energy were presented.

The quantum mechanical SG potential (the Mathieu potential) is the basic element of condense matter theory. Tunneling from one minimum to the next, in the path integral formulation, is described by Euclidean classical paths – the instantons. The issues we discuss in this paper deal with quantum fluctuations around these paths. We would like to demonstrate by an explicit calculation how our tools work in this – well controlled and studied setting –before applying them to more complicated/realistic settings in quantum field theory. Therefore we do *not* use anything stemming from the Schrödinger equation in this work, in particularly do not use series resulting from recurrence relations or resurgence relations (in general, conjectured) by several authors.

One reason to study SG is to explore further the existing deep connections between the quantum mechanical instantons – via Schrödinger equation – with wider mathematical issues, of approximate solutions to differential equations, defined in terms of certain generalized series. A particular form of an exact quantization condition was *conjectured* by Zinn-Justin [5], which links series around the instantons with the usual perturbative series in the perturbative vacuum. It remains unknown whether it can or cannot be generalized to the field theory cases we are mainly interested in. Recently, for the quartic double well and Sine-Gordon potentials Dunne and Ünsal (see [6] and also references therein) have presented more arguments for this connection, which they call *resurgent relation* between perturbative and instanton sectors.

Another reason for which we decided to do this work is a certain set of observations about

Feynman diagrams on top of the instanton for the double well potential with degenerate minima we observed in our first paper [1]. We wanted to see how general they are, using another example, now with infinitely many degenerate minima. The SG potential also has new vertices and thus many new diagrams. As we will show below, indeed all these trends repeat themselves in this second setting as well.

Few comments on the history of present approach. Omitting well known classic papers on instanton calculus we mention a pioneering paper [7], where the two-loop correction to the tunneling amplitude for the SG was calculated. In particular, the formalism for treating the zero-mode singularities was described in detail.

Three-loop correction to the instanton density

Let us consider the quantum-mechanical problem of a particle of mass $m = 1$ in the Sine-Gordon potential

$$V \;=\; \frac{1}{g^2}[\,1-\cos(g\,x)\,]\;. \tag{1}$$

The well-known instanton solution $X_{inst}(t) \;=\; \frac{4}{g}\arctan(e^t)$ describes the tunneling between adjacent minima is the classical path with the action $S_0 = S[X_{inst}(t)] = \frac{8}{g^2}$. Our notation for the coupling is related to those used in [5] by $g_{ZJ} = \frac{g^2}{16}$. The classical action S_0 of the instanton solution is therefore large and $\frac{1}{S_0}$ is used in the expansion.

The SG potential has an infinite number of degenerate minima, and perturbative levels in them form a continuous band, with states within the band labeled by Bloch angular parameter θ. The energy of the lowest band is

$$E_\theta^{(\text{lowest band})} \;=\; E_0 - \frac{\delta\,E}{2}\,\cos\theta\;, \tag{2}$$

where E_0 is the naive ground state energy, without tunneling, written as the following expansion

$$E_0 \;=\; \frac{1}{2}\sum_{n=0}^{\infty}\frac{A_n}{S_0^n} \quad , \qquad (A_0=1)\;, \tag{3}$$

while $\delta\,E \;=\; E_{\theta=\pi}^{(\text{lowest band})} - E_{\theta=0}^{(\text{lowest band})}$ generates another series, related to the so called instanton density

$$\delta\,E \;=\; \Delta E\sum_{n=0}^{\infty}\frac{B_n}{S_0^n} \quad , \quad (B_0=1)\;, \tag{4}$$

here $\Delta E = 2\sqrt{\frac{2\,S_0}{\pi}}\,e^{-S_0}$ is the well-known one-loop semiclassical result [7]. Coefficients A_n in the series (3) can be calculated using the ordinary perturbation theory (see [8]) while many coefficients B_n in the expansion (4) were found by Zinn-Justin, 1981-2005 (see [5] and references therein), obtained via the so called *exact Bohr-Sommerfeld quantization condition*. Alternatively, using the Feynman diagrams technique Lowe and Stone [7] calculated the two-loop correction $B_1 = -56/64$ which was later on reproduced by Zinn-Justin [5] in the so-called *exact Bohr-Sommerfeld quantization* technique. Higher order coefficients B_n in (4) can also be computed in this way. Since we calculate the energy difference, all Feynman diagrams in the instanton background (with the instanton-based vertices and the Green's function) need to be accompanied by subtraction of the same diagrams for the trivial $x = 0$ saddle point (see [9] for details). For $\frac{1}{\Delta E} \gg \tau \gg 1$ it permits to evaluate the ratio

$$\frac{\langle\, \pi\, |e^{-H\,\tau}|0\,\rangle_{x=X_{inst}}}{\langle\, 0\, |e^{-H\,\tau}|0\,\rangle_{x=0}}$$

where the matrix elements $\langle\pi|e^{-H\,\tau}|0\rangle_{x=X_{inst}}$, $\langle 0|e^{-H\,\tau}|0\rangle_{x=0}$ are calculated using the instanton-based Green's function and the Green function of the harmonic oscillator, respectively.

The instanton-based Green's function $G(x,y)$ form to be used

$$\begin{aligned} G(x,y) \;&=\; \frac{G^0(x,y)}{2\,(1+x^2)(1+y^2)}\Big[1 + 4\,x\,y + x^2\,y^2 + x^2 + y^2 \\ &\quad + (1 - 4xy + x^2y^2 + x^2 + y^2 + 2(1-xy)|x-y|)\log(2\,G^0(x,y))\Big]\;, \end{aligned} \tag{5}$$

is expressed in variables $x = \tanh(\frac{t_1}{2})$, $y = \tanh(\frac{t_2}{2})$, in which the familiar Green function $\frac{1}{2}e^{-|t_1-t_2|}$ of the harmonic oscillator is

$$G^0(x,y) \;=\; \frac{1 - |x-y| - x\,y}{2(1 + |x-y| - x\,y)}\;, \tag{6}$$

In its derivation there were two steps. One was to find a function which satisfies the Green function equation, used via two linearly-independent solutions and standard Wronskian method. The second step is related to a zero mode: one can add a term $\phi_0(t_1)\phi_0(t_2)$ with any coefficient and still satisfy the equation. The coefficient is then fixed from orthogonality to the zero mode.

The two-loop coefficient in (4) is [7]

$$B_1 = a + b_1 + b_2 + c\;,$$

$$a = -\frac{53}{60}, \qquad b_1 = \frac{3}{40}\ , \qquad b_2 = \frac{7}{20}\ , \qquad c = -\frac{5}{12}\ . \tag{7}$$

reflecting the contribution of four Feynman diagrams, see Fig. 1.

The three-loop correction B_2 (4) we are interested in is given by the sum of twenty-two 3-loop Feynman diagrams, which we group as follows (see Figs. 2 - 3)

$$\begin{aligned} B_2 \ &= a_1 + b_{11} + b_{12} + b_{21} + b_{22} + b_{23} + b_{24} \\ &\quad + d + e + f + g + h + j + k + l + c_1 + c_2 + c_3 + c_4 + c_5 + c_6 + c_7 + B_{2loop}\ , \end{aligned} \tag{8}$$

complementing by a contribution from two-loop Feynman diagrams, see Fig. 1,

$$B_{2loop} \ = \ \frac{1}{2}(a + b_1 + b_2)^2 + (a + b_1 + b_2)\, c \ = \ \frac{341}{1152}\ ,$$

(see (7)).

The rules of constructing the integrals for each diagram should be clear from an example: the explicit expression for the Feynman integral b_{23} in Fig. 2, which is

$$b_{23} = 32768 \int_{-1}^{1} dx \int_{-1}^{1} dy \int_{-1}^{1} dz \int_{-1}^{1} dw\, J(x,y,z,w) \left(x\, y\, z\, w\, G_{xx} G_{xy} G_{yz} G_{yw} G_{zw}^2 \right)\ , \tag{9}$$

while for c_4 in Fig. 3 it takes the form

$$c_4 = 256 \int_{-1}^{1} dx \int_{-1}^{1} dy \int_{-1}^{1} dz \frac{x\, y\, (1 - 6z^2 + z^4)}{(1+x^2)^2 (1+y^2)^2 (1+z^2)^2 (1-z^2)}\, G_{xy}\, G_{yz}^2\, G_{zz}\ , \tag{10}$$

here we introduced notations $G_{xy} \equiv G(x,y)$, $G^0_{xy} \equiv G^0(x,y)$ and $J = \frac{1}{(1+x^2)^2} \frac{1}{(1+y^2)^2} \frac{1}{(1+z^2)^2} \frac{1}{(1+w^2)^2}$. Notice that the c´s diagrams come from the Jacobian of the zero mode and have no analogs in the perturbative vacuum problem.

Results

The obtained results are summarized in Table I. All diagrams are of the form of one-dimensional, two-dimensional, three-dimensional and four-dimensional integrals. The five diagrams b_{11}, d, k, l, c_7, in particular (see Fig. 2)

$$\begin{aligned} b_{11} \ &= \ \frac{16}{3} \int_{-1}^{1} dx \int_{-1}^{1} dy\, \frac{1}{(1-x^2)(1-y^2)} \left(\frac{(1 - 6x^2 + x^4)(1 - 6y^2 + y^4)}{(1+x^2)^2 (1+y^2)^2}\, G_{xy}^4 - (G^0_{xy})^4 \right) \\ d \ &= \ 16 \int_{-1}^{1} dx \int_{-1}^{1} dy\, \frac{1}{(1-x^2)(1-y^2)} \\ &\qquad \left(\frac{(1 - 6x^2 + x^4)(1 - 6y^2 + y^4)}{(1+x^2)^2 (1+y^2)^2} G_{xx} G_{xy}^2 G_{yy} - G^0_{xx} (G^0_{xy})^2 G_{yy} \right)\ , \end{aligned} \tag{11}$$

correspond to two-dimensional integrals and together with diagram j, a one-dimensional integral, are the only ones which we are able to calculate analytically

$$\begin{aligned} b_{11} &= -\frac{189199}{756000} + \frac{1}{900}\Big(178\,\zeta(2) - 204\,\zeta(3) + 27\,\zeta(4)\Big) \equiv b_{11}^{rat} + b_{11}^{irrat} \\ d &= -\frac{73931}{47250} + \frac{289}{900}\zeta(2) \equiv d^{rat} + d^{irrat} \ , \\ j &= \frac{184}{315} \ , \qquad k = -\frac{379}{630} \ , \qquad l = -\frac{244}{945} \ , \qquad c_7 = \frac{16}{45} \ , \end{aligned} \tag{12}$$

here $\zeta(n)$ denotes the Riemann zeta function of argument n (see [10]). Diagrams b_{11}, d, contain a rational and an irrational contribution such that

$$\frac{b_{11}^{irrat}}{b_{11}^{rat}} \approx -0.341 \qquad , \qquad \frac{d^{irrat}}{d^{rat}} \approx -0.338 \ .$$

It shows that for diagrams b_{11} and d the rational contribution is three times larger than the irrational part. In the case of the DW potential the situation is opposite, the irrational part is dominant (see [1]). Other diagrams, see Table I, were evaluated numerically with an absolute accuracy $\sim 10^{-7}$. Surprisingly, almost all of them (20 diagrams out of 22 ones in total) are of order $\geq 10^{-1}$ as for B_2 itself with two of them (diagrams b_{12}, b_{21}) which are of order 10^{-2}.

J. Zinn-Justin (see [5] and references therein) reports a value of

$$B_2^{Zinn-Justin} = -\frac{59}{128} \approx -0.4609375 \ , \tag{13}$$

while present calculation shows that

$$B_2^{present} \approx \ -0.4609377 \ , \tag{14}$$

which is in agreement, up to the precision employed in the numerical integration.

Similarly to the two-loop correction B_1 the coefficient B_2 is negative. For not-so-large barriers ($S_0 \sim 1$), the two-loop and three-loop corrections are of the same order of magnitude. The dominant contribution comes from the sum of the two-vertex diagrams $d, b_{11}, k, l, c7$ while the four-vertex diagrams $b_{12}, b_{21}, b_{23}, e, h, c_1, c_5, c_6$ provides minor contribution, the absolute value of their sum represents less than 0.2% of the total correction B_2. Interesting that for both two and three loop cases the largest contribution comes from the 'ears'-like diagrams a and d, respectively, $\frac{a}{B_1} \approx 1.01$ and $\frac{d}{B_2} \approx 2.25$.

We already noted that individual three-loop diagrams contain irrational numbers. If J. Zinn-Justin´s rational result is correct, then there must be a cancelation of these irrational contributions in the sum (8). From (12) we note that the term $(b_{11}^{irrat} + d^{irrat})$ gives a contribution of order one to the mentioned sum (8), and therefore the coincidence in the order of 10^{-7} between present result (14) and one of Zinn-Justin (13) is an indication that such a cancelation occurs. Now, we evaluate the coefficients A_1, A_2 in (3) using Feynman diagrams (see [8]). In order to do it let us consider the Sine-Gordon potential $V = \frac{1}{g^2}[\,1 - \cos(g\,x)\,]$ and calculate the transition amplitude $\langle x = 0|e^{-H\,\tau}|x = 0\rangle$. All involved Feynman integrals can be evaluated analytically. In the limit $\tau \to \infty$ the coefficients of order S_0^{-1} and S_0^{-2} in front of τ gives us the value of A_1 and A_2, respectively. As it was mentioned above the $c\,´s$ diagrams do not exist in this case. The Feynman integral a in Fig. 1 give us the value of A_1, explicitly it is equal to

$$A_1 = -2\ .$$

The diagrams b_{11}, d and j in Fig. 2 determine A_2, $b_{11} = -\frac{4}{3}\ d = -8$ and $j = \frac{16}{3}$. Then

$$A_2 = -4\ ,$$

which is in agreement with the results obtained in standard multiplicative perturbation theory (see e.g. [11]). No irrational numbers appear in the evaluation of A_1 and A_2.

Conclusions and Discussion

In conclusion, we have calculated the tunneling amplitude (level splitting related to the instanton density) up to three-loops using Feynman diagrams for quantum perturbations on top of the instanton. Summing all of these contributions we obtain the third coefficients B_2 (defined in (4)). The result – to the numerical accuracy we kept – is found to be in good agreement with the resurgent relation between perturbative and instanton series suggested by Zinn-Justin (for modern reference see [5]).

Let us remind again, that this paper is methodical in nature, and its task was to develop tools to calculate tunneling phenomena in multidimensional QM or QFT context, in which any results stemming from Schrödinger equation are not available. We use a quantum mechanical example as a test of the tools we use: but the tools themselves are expected to work in much wider context.

When we started these works (see [1]) we, naively, expected to see some correspondence between vacuum and instanton series on the level of individual Feynman diagrams. However, no such trend has been detected so far. Furthermore, "new" diagrams originating from the instanton zero mode Jacobian, surprisingly, provide the dominant contribution ($\sim 114\%$) to the three-loop correction B_2, see Table I, both for 2-loop and 3-loop contributions, both for the double well and SG problems. In the double well case the "new" individual diagrams c and c_5 give the dominant contribution (83% and 126%) to the overall loop coefficients B_1 and B_2 out of 4 and 18 diagrams, respectively, while in the SG case they give significant contributions 48% and 25% out of 4 and 22 diagrams, respectively. (However, the corresponding c_5-like four-loop diagram in the SG case represents the 4% of the four-loop correction B_3 only.)

Another observation is that the final three-loops answer has a rational value. However, unlike the evaluation of the two-loop coefficient B_1 where all Feynman diagrams turned out to be rational numbers, in our case of B_2 at least two diagrams contain irrational parts. What is the origin of these terms and how they cancel out among themselves are questions left unanswered above, since several diagrams had resisted our efforts to get the analytic answer, so that we used numerical integration methods. Perhaps this can still be improved.

Similar calculations for scalar and eventually gauge theories would be certainly possible and are of obvious interest. The diagrams are the same, and the basic element remains explicit Green functions. (In the case of gauge theories those should be orthogonal to all –including gauge– zero modes.)

Acknowledgments

MAER is grateful to J.C. López Vieyra for assistance with computer calculations. This work was supported in part by CONACYT grant **166189** (Mexico) for MAER and AVT, and also by DGAPA grant IN108815-3 (Mexico) for AVT. The work of ES is supported in part by the U.S. Department of Energy under Contract No. DE-FG-88ER40388.

---

[1] M.A. Escobar-Ruiz, E. Shuryak, A.V. Turbiner, *Three-loop Correction to the Instanton Density. I. The Quartic Double Well Potential*,

arXiv:1501.03993v2

[2] A. C. Scott, F. Y. F. Chu, and D. W. McLaughlin, *Proc. IEEE* **61**, 1443 (1973)

[3] S. Coleman, *Phys. Rev. D* **11**, 2088-2097 (1975)

[4] J.-Q. Liang and H. J. W. Miiller-Kirsten, *Phys. Rev. D* **51**, 718-725 (1995)

[5] J. Zinn-Justin and U.D. Jentschura, *Annals Physics* **313**, 269-325 (2004)
quant-ph/0501137 (updated, February 2005)

[6] G. V. Dunne and M. Ünsal, *Phys. Rev. D* **89**, 105009 (2014)

[7] M. Lowe and M. Stone, *Nucl. Phys. B* **136**, 177-188 (1978)

[8] C. M. Bender and T. T. Wu, *Phys. Rev.* **184**, 1231-1260 (1969)

[9] A. A. Aleinikov and E. Shuryak, *Sov. J. Nucl. Phys.* **46**, 76 (1987)

[10] E.T. Whittaker and G.N. Watson, *A Course in Modern Analysis*
4th edition, Cambridge University Press, 1927

[11] A. V. Turbiner, *JETP Lett.* **30**, 352-355 (1979) (English Translation) [Soviet Phys. – Pisma ZhETF **30**, 379-383 (1979)].

Feynman diagram	Contribution to B_2
a_1	0.07649737
b_{12}	0.01201803
b_{21}	0.02179546
b_{22}	0.1266254
b_{23}	0.08934351
b_{24}	0.1367672
e	0.09567712
f	0.3168478
g	0.3089885
h	0.06178483
c_1	-0.05369549
c_2	-0.3472822
c_3	-0.07161299
c_4	-0.1830249
c_5	-0.1149061
c_6	-0.1112634
I_{2D}	-1.70563
I_{3D}	0.36380
I_{4D}	0.00075

Table I: Contribution of diagrams in Fig. (2)-(3) for the three-loop correction B_2. We write $B_2 = (B_{2loop} + I_{1D} + I_{2D} + I_{3D} + I_{4D})$ where $j = I_{1D}$ and I_{2D}, I_{3D}, I_{4D} denote the sum of two-dimensional, three-dimensional and four-dimensional integrals, respectively. The term $B_{2loop} = 341/1152 \approx 0.296$ (see text).

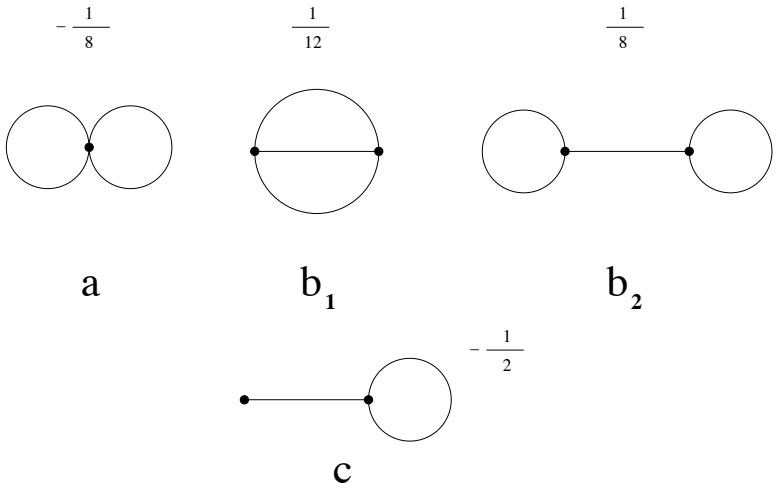

Figure 1: Diagrams contributing to the two-loop correction $B_1 = a+b_1+b_2+c$. They enter into the coefficient B_2 via the term B_{2loop}. For the instanton field the effective triple, quartic, quintic and sextic vertices are $V_3 = 4\sqrt{2}\,\frac{\sinh(t)}{\cosh^2(t)}\,S_0^{-1/2}$, $V_4 = 8\,(2/\cosh^2(t)-1)\,S_0^{-1}$, $V_5 = -32\sqrt{2}\,\frac{\sinh(t)}{\cosh^2(t)}\,S_0^{-3/2}$, $V_6 = -64\,(2/\cosh^2(t)-1)\,S_0^{-2}$, respectively, while for the subtracted vacuum field diagrams we have $V_3 = V_5 = 0$, $V_4 = 8\,S_0^{-1}$ and $V_6 = 64\,S_0^{-2}$. The tadpole in diagram c, which comes from the zero-mode Jacobian rather than from the action, is effectively represented by the vertex $V_{tad} = \frac{1}{\sqrt{2}}\frac{\sinh(t)}{\cosh^2(t)}\,S_0^{-1/2}$, (see text). The signs of contributions and symmetry factors are indicated.

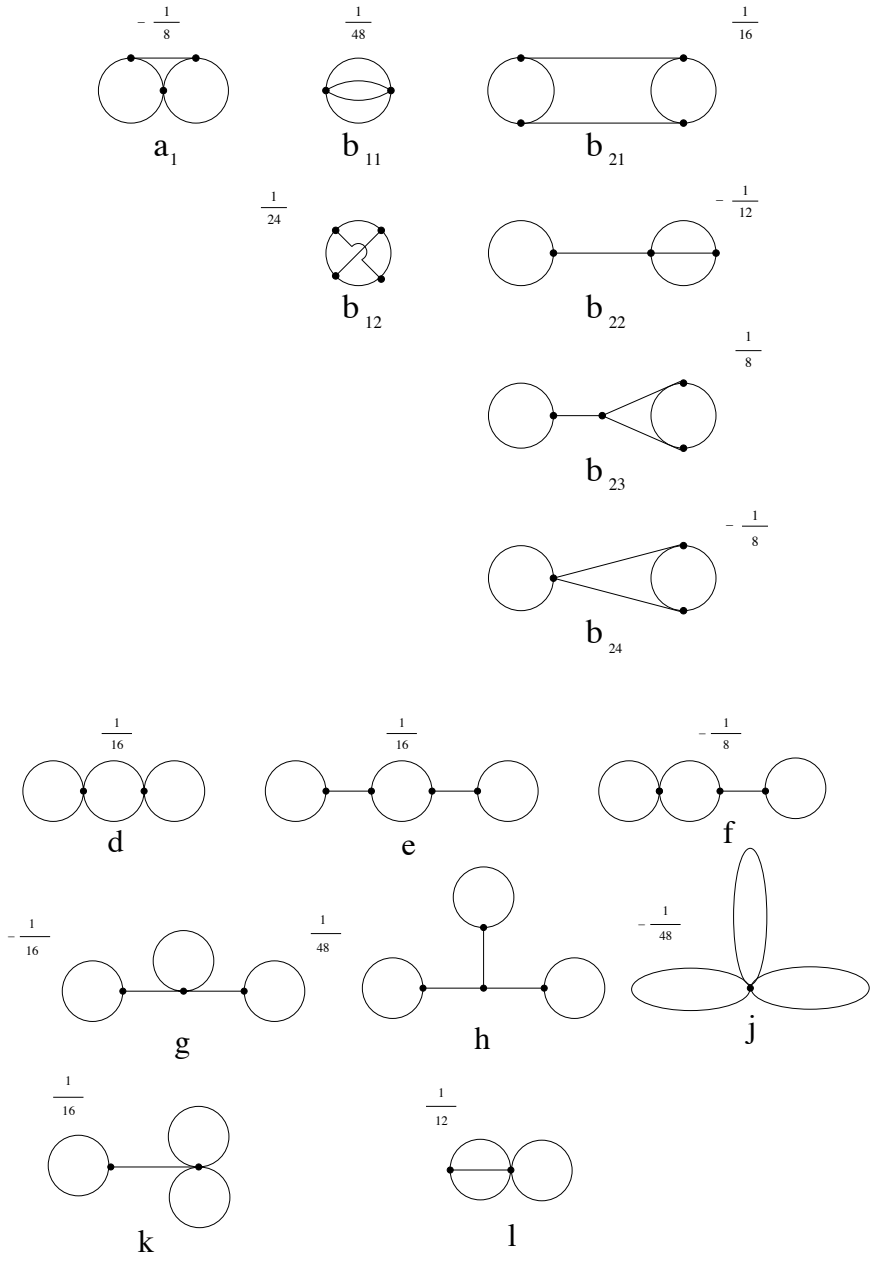

Figure 2: Diagrams contributing to the coefficient B_2. The signs of contributions and symmetry factors are indicated.

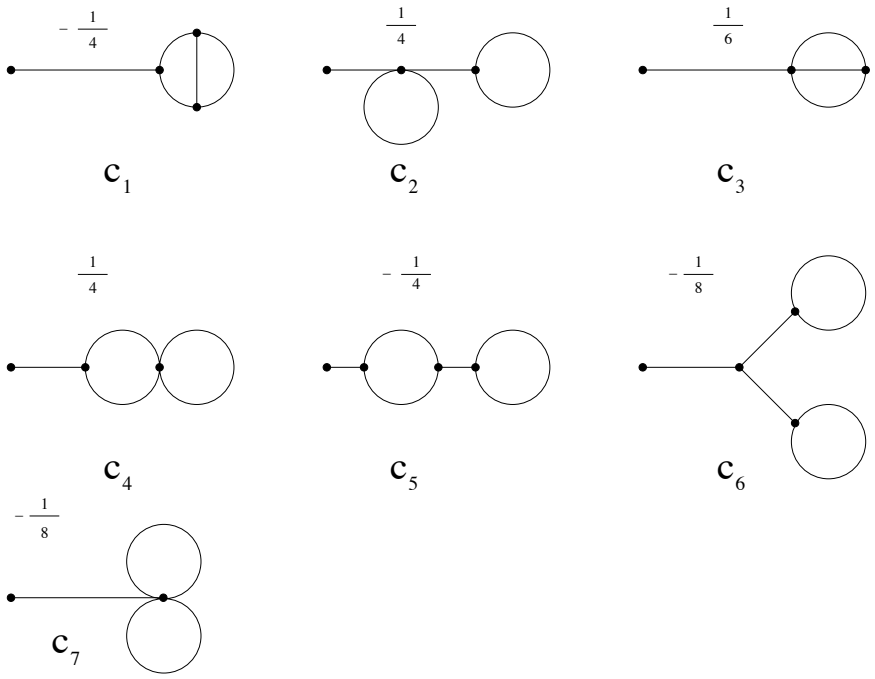

Figure 3: Diagrams contributing to the coefficient B_2. They come from the Jacobian of the zero mode and have no analogs in the perturbative vacuum. The signs of contributions and symmetry factors are indicated.